

## **Riverine impact on the thermohaline properties, turbidity and suspended solids in a shallow bay (Bay of Koper, northern Adriatic Sea)**

Rok SOCZKA MANDAC<sup>1\*</sup>, Branko BOGUNOVIĆ<sup>2</sup>, Dušan ŽAGAR<sup>3</sup> and  
Jadran FAGANELI<sup>4</sup>

<sup>1\*</sup> *Harpha sea, d.o.o. Koper, Čevljarska ulica 8, 6000 Koper, Slovenia*

<sup>2</sup> *Faculty of Mathematics, Natural Science and Information Technology,  
University of Primorska, Glagoljaška 8, 6000 Koper, Slovenia*

<sup>3</sup> *Faculty of Civil and Geodetic Engineering, University of Ljubljana, Jamova cesta 2, p.p. 3422,  
1000 Ljubljana, Slovenia*

<sup>4</sup> *Marine Biology Station, National Institute of Biology, Fornače 41, 6330 Piran, Slovenia*

*\*Corresponding author, e-mail: rok@harphasea.si*

---

*The influence of river discharge on the spatial and temporal variability of thermohaline and turbidity conditions at the sea surface (0.5 m) was studied in the shallow Bay of Koper (Gulf of Trieste, northern Adriatic Sea) which is influenced mainly by the polluted Rižana River. Conductivity, temperature and turbidity were measured monthly at 36 sampling sites between June 2011 and June 2013. Empirical orthogonal function analysis (EOF) was applied to investigate the data and to study the spatial distribution of variability and their temporal variations of temperature, salinity, density and turbidity. The EOF results showed an area of high variance in the proximity of the Rižana River mouth for all variables. The high variations in the time series for all variables were shown to be related mainly to high variations in the time series of the river discharges. Coupled field analysis showed the area of low salinity and high turbidity. A strong relationship was found between turbidity and suspended solid (TSS) concentration data collected in the local rivers and near shore zone suggesting that turbidity can be used as a satisfactory surrogate of TSS estimation.*

---

**Key words:** River discharge, thermohaline, turbidity, suspended solids, northern Adriatic Sea

### **INTRODUCTION**

The river input of fresh water exerts a significant impact on the thermohaline (TH) and turbidity properties of coastal waters (COZZI *et al.*, 2012). A high concentration of suspended solids is the

main cause of high turbidity in the estuary and adjacent coastal areas (WOLANSKI, 2007). Coastal ecosystems are sensitive to spatial and seasonal fluctuations of TH properties and turbidity (WOLANSKI, 2007). Strong horizontal and vertical gradients of TH properties are pronounced in

episodes of high river discharge, and coincide with high turbidity which is considered a stress factor for benthic organisms (ORPIN *et al.*, 2004). OGORELEC *et al.* (1987) suggested that the Rižana River is the major source of fluvial water and sediments flowing into the Bay of Koper (BoK), located in the eastern part of the Gulf of Trieste (northern Adriatic Sea). A sediment input rate of  $28 \cdot 10^3 \text{ t year}^{-1}$  was estimated by OGORELEC *et al.* (1987) from the mean river flow rate ( $4 \text{ m}^3\text{s}^{-1}$ ) and the averaged suspended sediment concentration ( $22 \text{ mg l}^{-1}$ ). The inflow of fluvial material is the principal cause of silting and the accumulation of a considerable quantity of sediments in the local port (Port of Koper) (LUKA KOPER, 2011). The coastal zone around the town of Koper is largely urbanized and industrialized and thus subjected to high anthropogenic pressures stemming from industry, port activities, marinas and tourism (ORLANDO BONACA *et al.*, 2008). Municipal and industrial waste waters, even if they are treated by industrial and municipal treatment plants, affect the Rižana and Badaševica Rivers (FAGANELI & TURK, 1989). Pollutants and nutrients are mostly bound through flocculation and adsorption on fluvial solids (COVELLI *et al.*, 2007; STONE & DROPPPO, 1996; DROPPPO, 2001) and transported by rivers into the BoK (TURK *et al.*, 2013; BAJT, 2000). Hence, the impact of the river Rižana is not limited to TH properties and turbidity but it also affects the distribution of TSS concentrations and associated nutrients and pollutants. The TSS concentration in the water column affects the light penetration influencing endangered species and habitats sensitive to light attenuation present in the BoK (LIPEJ *et al.*, 2006). Moreover, the particles of mud and sand can destabilize the substrate and bury the benthos (WOLANSKI, 2007). Methods which estimate total suspended solids concentration from turbidity data were studied in various environments (SUK *et al.*, 1998; GIPPEL, 1989; GIPPEL, 1995; HOFMANN & DOMINIK, 1995; PACKMAN *et al.*, 1999) and can be applied to study the relation between turbidity and TSS in the BoK, as well.

Spatial TH properties of the Gulf of Trieste have been described by MOSETTI (1967) and more recently by MALAČIČ *et al.* (2006). MALAČIČ *et al.* (2006) showed that Slovenian rivers, compared

with the Isonzo (Soča) River, play only a minor role in the variations of the TH properties of the Gulf of Trieste, so the main influence of the Rižana River, and to a much lesser extent of Badaševica River, is expected to be limited to the BoK area. The study of TH properties of BoK were also partially included in reports on bay sedimentology (OGORELEC *et al.*, 1987) and Rižana estuary pollution (FAGANELI & TURK, 1989). From the above literature it is assumed that the inflow of the Rižana River, with an annual discharge rate of  $\sim 4 \text{ m}^3\text{s}^{-1}$ , has a significant influence on spatial and temporal TH properties and on turbidity in the BoK but to a minor extent on the whole Gulf of Trieste.

This article presents spatial and temporal variations of TH properties, density and turbidity in the sea surface layer in the shallow BoK. The aims of this study were to:

- 1) Analyse spatial and temporal TH properties and turbidity variations in the BoK in relation to river discharge,
- 2) correlate spatial patterns and time series of salinity, density and turbidity,
- 3) determine the relationships between all studied variables along three vertical profiles,
- 4) evaluate whether turbidity data can be used as a satisfactory estimate of TSS in coastal waters.

In the prospective of the recently installed automatic hydrological station at the Rižana River (PRIMORSKE NOVICE, 2014) and the oceanographic buoys in the bay (LUKA KOPER, 2013; REGIONAL OBALA, 2014) the findings of this investigation provides a valid basis for further studies of TH and TSS.

## MATERIALS AND METHODS

### Study site

The BoK is a wide submerged valley of the Rižana River located in the Gulf of Trieste (northern Adriatic Sea) (OGORELEC *et al.*, 1991). It is a shallow, semi-enclosed bay with an average depth of 16 m, and covers about  $35 \text{ km}^2$  (OGORELEC *et al.*, 1987). The depth of BoK (Fig.1) decreases linearly from 23 m the open boundary

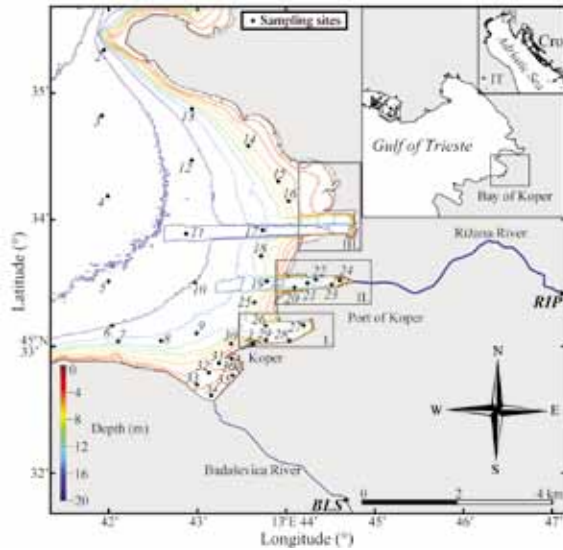


Fig. 1. Bay of Koper located in the Gulf of Trieste (northern Adriatic Sea). The contoured lines are the isobaths and the survey sites are numbered (1 - 36). The point BLS marks the sampling site on the Badaševica River and RIP on the Rižana River. The numbered squares (I, II, and III.) indicate the location of the port basins

of the bay on the west-side to 1m in the coastal zone. Three dredged canals (average depth 16 m) connect the open part of the gulf to the port basins (Fig. 1). The circulation is influenced mainly by tide (range of  $\pm 1$  m) and wind, in particular the easterly wind (Bora) (MALAČIČ *et al.*, 2014).

The mouth of the Rižana River is located on the east side of the BoK in the second basin of the port of Koper, while its relief outputs are located in the third basin of the port and in the brachial wetland zone of Škočjanski zatok. The first basin of the port of Koper is the most southern of the three port basins, situated in the vicinity of the town of Koper (Fig. 1). FAGANELI & TURK (1989) described the Rižana River as a small, polluted river with a variable mean flow rate of  $4 \text{ m}^3\text{s}^{-1}$  and the river estuary as being highly stratified, with a short mean fresh water replacement time of less than 1 day. The spatial distribution of fluvial water and particulate suspended matter (turbidity) in the BoK is affected by meteorological and hydrological factors, primarily wind (meteorological) and river discharge rate (hydrological), as well as maritime traffic (OGORELEC *et al.*, 1987; COV-

ELLI *et al.*, 2007). High discharges and sediment transport peaks occur during short periods of intense precipitation. The flow rate of the Rižana was recorded by the Slovenian Environmental Agency (ARSO) from 1966 to 2013 at the gauge station Kubed (located 13 km upstream from the river mouth), and that of the Badaševica River at Šalara (located 3.2 km upstream from the river mouth). The mean water flow of the Rižana between 1966 and 2012 was  $3.9 \text{ m}^3\text{s}^{-1}$  (ARSO, 2014 c), minimum discharge  $\sim 0.1 \text{ m}^3\text{s}^{-1}$  and maximum of  $190.5 \text{ m}^3\text{s}^{-1}$  recorded during an extreme event in 2010. The Badaševica River has a lower flow rate, with a minimum  $\sim 0.1 \text{ m}^3\text{s}^{-1}$  and a maximum flow rate of  $6.2 \text{ m}^3\text{s}^{-1}$  (an extreme event in 2006); the annual mean discharge is  $0.3 \text{ m}^3\text{s}^{-1}$  (ARSO, 2014 c). Additionally, it was observed that the discharge of the two local rivers can increase up to ten times within a few hours (PLUT, 1980). Other inputs of fresh water in the BoK are runoffs of storm water located around the bay. The discharge of these runoffs is not measured and therefore not included in the analysis. The meteorological data were measured in the port zone (lon =  $13.7^\circ$  ; lat =  $45.6^\circ$  ; height = 2 m) by the ARSO meteorological station (ARSO, 2014 b).

### Field measurements, sampling and TSS concentration measurements

Campaigns were performed at 36 survey and sampling sites in the BoK (Fig. 1), between June 2011 and June 2013 (28 campaigns) at monthly intervals. In order to avoid episodes of sediment re-suspension induced by maritime traffic, the survey was performed during low maritime traffic. The water column was profiled using a conductivity, temperature and depth (CTD) probe (Hydrolab data sonde model 4a) with turbidity sensor (ISO 7027 compliant) which measures the light back scatters within a wave light of  $860\text{nm} \pm 10\text{nm}$ . Before each cast, the instrument was allowed to stabilize for 1 minute. The probe was lowered manually from the water surface to the sea bed, recording temperature, conductivity and turbidity data at the sampling rate of 1 Hz. The depth interval for the input data of variables was chosen between 0.2 – 0.7 m, which

is denoted as the sea surface layer (SSL) 0.5 m. Water samples for TSS were collected at the surface (0.5 m deep) at 19 sampling sites in the bay, one at the Rižana River mouth and at 2 sampling sites in the Rižana (RIP) and Badaševica (BLS) Rivers (Fig. 1) using 10 l Niskin samplers. The water samples (1 l) were immediately stored in polyethylene bottles at 5°C and filtered within four hours. One litre of water sample was filtered through a pre-weighed 47 mm diameter Whatman GF/F glass-fibre filter with approximately 0.7 µm pores pre-ignited at 480°C for 3 hours. The filters with particles were washed several times with MiliQ water to remove salt and dried at 60°C in an oven (Aurodent typ 830 nf). TSS concentration was determined gravimetrically and suspended organic matter (SOM) concentration gravimetrically after combustion in a 480°C furnace for 2 hours.

### Quality checking and data processing

Probe calibration was tested with standard solutions before and at the end of the measurement campaigns. Before data processing, the temperature (°C), salinity in practical salinity units (PSU) and turbidity in Nephelometric Turbidity Units (NTU) profiles were controlled by a data quality check (4°C < Temperature < 33°C ; 8 PSU < Salinity < 40 PSU; 0 NTU < Turbidity < 400 NTU). Sea water density was calculated at atmospheric pressure using the UNESCO 1983 (EOS 1980) polynomial equation (FOFONOFF *et al.*, 1983). Horizontal natural neighbour interpolation (LEDOUX & GOLD, 2005) was used to provide spatial grid maps of the sea surface variables of 514×342 cells and ~ 10×10 m cell resolution. The empty cells were excluded in order to avoid errors in the further analysis.

### Empirical orthogonal function analysis

The EOF method (PREISENDORFER & MOBLEY, 1988) is a statistical tool used in many branches of science, among others meteorology and oceanography, to identify spatial patterns of variability and to measure the statistical importance of each pattern and of its time variation (BJÖRNSSON & VENEGAS, 1997). Examples of the

use of EOF can be found in the research into Black Sea surface temperature (BUONGIORNO NARDELLI *et al.*, 2010) and seasonal and inter-annual variations of sea surface salinity in the tropical Pacific Ocean (DELCROIX & HÉNIN, 1991). The EOF aims to cast a single variable in terms of space and time and is a useful method for studying large quantities of data (GLOVER *et al.*, 2011). Before proceeding with the EOF and coupled field analysis, the domain of the third basin (see Fig. 1) was excluded from the analysis due to lack of data in this part of the BoK. The grid maps of the sea surface (SSL<sub>p</sub>) for studied variable indexed (*p*) were reshaped in the S-mode (the maps were organized column-wise) matrix  $X_p$  of size  $N \times M$  ( $N$  (SSL) time slice (*t*) and  $M$  grid cells (SSL)) in accordance with the specification of GLOVER *et al.* (2011). The mean value of data was removed and formed a covariance matrix ( $R_p$ ) (GLOVER *et al.*, 2011):

$$R_p = X_p (t)' X_p (t) / (N - 1) \quad (2.1)$$

The eigenvectors called patterns ( $EOF_p$ ) and eigenvalues ( $\delta_p$ ) were extracted using the function eig.m provided by GLOVER *et al.* (2011), and the EOF loadings or spatial EOFs amplitude calculated from:

$$X_p = \sum_{k=1}^N b_{pk}(t) EOF_{pk} \quad (2.2)$$

coefficients, called amplitudes ( $b_p(t)$ ), are calculated as weighted linear combinations of the data grid points:

$$b_{pk}(t) = EOF_{pk} X_{pk}(t) \quad (2.3)$$

and the percentage of covariance ( $PoV$ ) is calculated from eigenvalues of leading *k*-modes:

$$PoV_{pk} = \frac{\delta_{pk}}{\sum_{k=1}^N \delta_{pk}} \quad (2.4)$$

### Coupled fields methods

In order to identify the relationship between the studied variables, EOF analysis can be extended to a comparison of the time-evolution of the two property distributions (GLOVER *et al.*,

2011). In the literature (BRETHERTON *et al.*, 1992), these techniques are also called singular value decomposition (SVD) (BJÖRNSSON & VENEGAS, 1997), and constitute one of the approaches that isolate coupled modes of variability between time series of two fields. The coupled field method is used to study correlation maps for the  $k$ -th mode, defined as the vectors of correlation values between the expansion coefficient of  $k$ -th mode of a field at each grid point (BRETHERTON *et al.*, 1992; BJÖRNSSON & VENEGAS, 1997).

The cross-covariance matrix ( $R_{lr}$ ) is formed from two maps ( $X_p$ ) indexed with  $l$  – left and  $r$  – right as:

$$R_{lr} = X_{pl}(t)' X_{pr}(t) \quad (2.5)$$

The singular vectors and singular values are extracted using the fundamental matrix operation SVD (BJÖRNSSON & VENEGAS, 1997; GLOVER *et al.*, 2011):

$$R_{lr} = USV' \quad (2.6)$$

$U$  contains the left and  $V$  the right patterns (eigenvectors) of  $R_{lr}$ , while the  $S$  contains the singular values ( $S_k$ ) of  $R_{lr}$ , (BJÖRNSSON & VENEGAS, 1997; GLOVER *et al.*, 2011). The time series are computed with:

$$R_l = X_{pl}U \quad (2.7)$$

$$R_r = X_{pr}V \quad (2.8)$$

To address the relative importance of the  $k$ -th mode the squared covariance fraction (SCF) is defined (BJÖRNSSON & VENEGAS, 1997) as follows:

$$SCF = \frac{S_k^2}{\sum_{j=1}^N S_j^2} \quad (2.9)$$

### Factor analysis

Factor analysis (FA) is a statistical extension of principal component analysis which is described in detail by GLOVER *et al.* (2011). FA defines the more important and retained factors containing the “signal” and the less important factors containing the “noise” (GLOVER *et al.*,

2011). The covariance matrix was constructed in Q-mode form (variables are oriented row wise) from three different profiles, performed at measurement sites 5, 19 and 24 (Fig.1) incorporating temperature, salinity, turbidity and calculated density. The data were standardized and the eigenvalue and the singular value extracted from the covariance matrix using the eigsort.m computation (GLOVER *et al.*, 2011).

## RESULTS AND DISCUSSION

### Field data

Spatial maps (28) for all variables in the SSL were averaged in time (in the studied period June 2011 to June 2013) and the results (Fig. 2) show the influence of the river mainly in the proximity of the Rižana River mouth. Obviously the temperature in the SSL is mainly related to the annual cycle of solar radiation (MALAČIČ *et al.*, 2006) which is assumed to be uniformly distributed spatially if the influence of clouds is disregarded. However, the average temperature (Fig. 2a) in the second basin was 17.4°C and in the central part of the bay 18.3°C, while an overall maximum temperature of 18.6°C was observed in the shallow part. The salinity (Fig. 2b) in the second port basin was 28 PSU (minimum) and in the western part, 36.5 PSU (maximum). The same spatial distribution was observed in the density pattern (Fig. 2c) with a strong horizontal density gradient  $\Delta\rho = 6 \text{ kgm}^{-3}/\text{km}$ . Thus, the averaged SSL density structure is affected mainly by river discharge. The horizontal gradient of turbidity (Fig. 2d) in the SSL is  $\Delta\text{Turbidity} = 8 \text{ NTU}/\text{km}$ , with minima of 1 NTU in the south part, 3 NTU in the central part of the bay and maximum (mean) of 11 NTU in the second basin. A similar structure pattern is present on all variable maps, confirming the significant influence of riverine inflow on coastal water during the studied period.

At the beginning of the studied period several precipitation episodes occurred. The average daily precipitation between 1<sup>st</sup> June and 6<sup>th</sup> June 2011 was 0.5 mm (see Fig. 3); the maximum 16

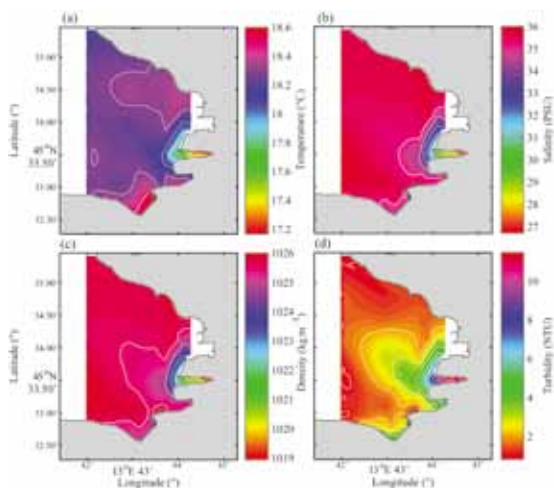


Fig. 2. Average SSL temperature (a), salinity (b), density (c) and turbidity (d) horizontal distribution interpolated from 36 survey sites for the 28 survey campaigns in the 2011 - 2013 period

mm was observed on 6<sup>th</sup> June 2011 (ARSO, 2014 b). During this month surveys were intensified (Fig. 3) in order to record the high river discharge event. The highest horizontal and vertical stratification for all variables in the period studied was observed on 8<sup>th</sup> June 2011, related

to high fresh water discharge of the Rižana (maximum  $31 \text{ m}^3\text{s}^{-1}$ ) and Badaševica (maximum  $2 \text{ m}^3\text{s}^{-1}$ ) Rivers (ARSO, 2014 c). A horizontal temperature gradient ( $\Delta T = 6^\circ\text{C} / \text{km}$ ) was noted between the mouth of the Rižana River and the centre of the BoK. Salinity and turbidity gradients were evaluated at the boundary of the front -  $\Delta S = 20 \text{ PSU}/\text{km}$  and  $\Delta \text{Turbidity} = 120 \text{ NTU}/\text{km}$ . An extremely dry period occurred between October 2011 and October 2012 (Fig. 3) and a climatological (1955-2013) minimum discharge of the Rižana River (mean  $1.9 \text{ m}^3\text{s}^{-1}$ ) was recorded (ARSO, 2014 c). Twelve days of dry and cold, with Bora wind speed  $> 15 \text{ m s}^{-1}$  in February 2012 (ARSO, 2014 b) resulted in homogenization of the entire water column (ARSO, 2012 a). During this period, minimum temperature  $4^\circ\text{C}$  and maximum salinity  $38.7 \text{ PSU}$  were recorded along the water column. Between August 2012 and June 2013 the frequency of precipitation increased, resulting in an average precipitation  $> 0.1 \text{ mm}$  and an average river flow rate of  $5.9 \text{ m}^3\text{s}^{-1}$ . The average river flow rate during the surveys was  $4.6 \text{ m}^3\text{s}^{-1}$ , slightly higher than

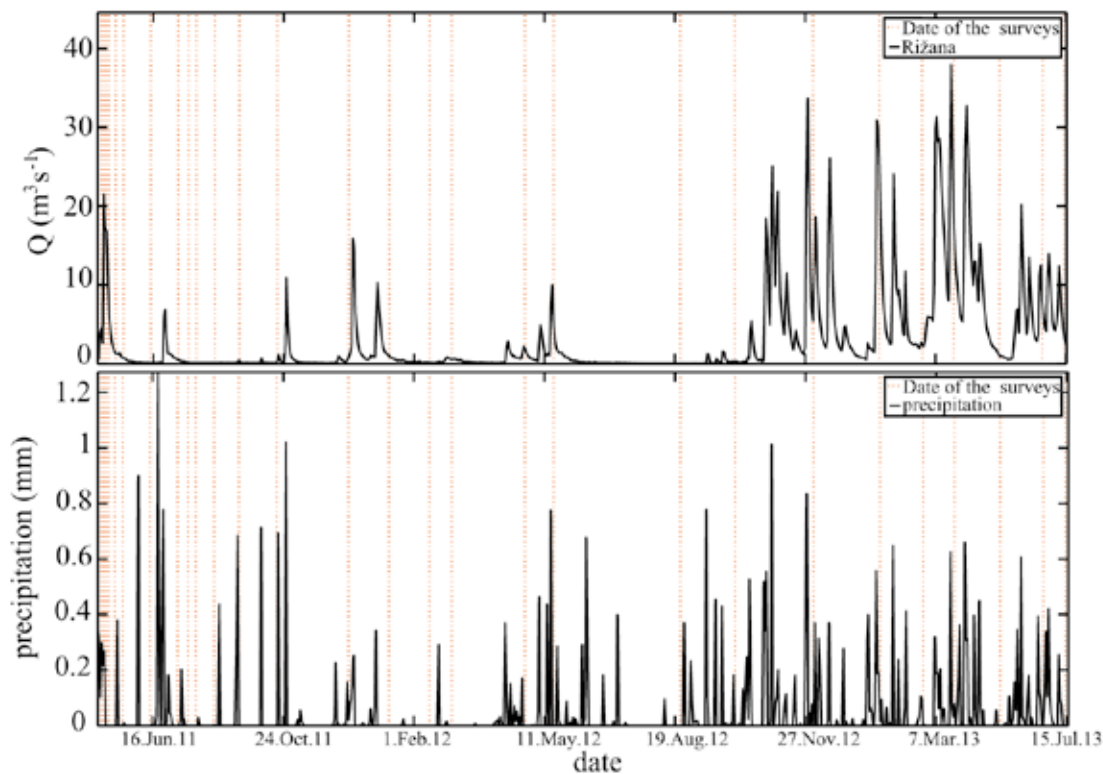


Fig. 3. Mean river flow of the Rižana River and mean precipitation in the period June 2011- June 2013

the  $3.9 \text{ m}^3\text{s}^{-1}$  (ARSO, 2014 c) recorded during the climatological period. Two different stages of the Rižana River discharge were recorded during the studied period, low discharge  $1.1 \text{ m}^3\text{s}^{-1}$  (between 6<sup>th</sup> June 2011 and 6<sup>th</sup> June 2012) and high discharge  $5.1$  (between 6<sup>th</sup> June 2012 and 6<sup>th</sup> June 2013) (ARSO, 2014 c).

### EOF analysis

Most of the explained variance lies in the first mode: temperature 99%, turbidity 77%, density 73% and salinity 69% (see Fig. 4). Modes explaining less than  $\sim 20\%$  of the variance showed the spatial structure of the EOF and expansion coefficients that were not related to the hydrological impact and were excluded from further analysis. The following spatial maps and expansion coefficients are normalized on scale 0 – 1 in accordance with BJÖRNSSON & VENEGAS (1997).

#### EOF analysis of temperature and salinity

Spatial distribution of the first mode (Fig. 5a), shows lower amplitude signal in the region close to the Rižana River mouth. The amplitude of the signal decreases from the open part of the bay (0.8) to the Rižana River mouth (0) which suggests a cooling/heating action of the fresh water inflow. A rather less pronounced signal amplitude ( $\sim 0.6$ ) was observed at the western boundary of the BoK suggesting variations related to the exchange of water masses with the rest of the Gulf of Trieste. The maximum value was observed in the vicinity of the Badaševica river mouth and in the north-eastern

part of BoK. This variability is associated with the interaction between the air and the relatively confined water mass in the shallow zone ( $\sim 1.5$  m). The expansion coefficient of the first mode (Fig. 6a) shows the signal of seasonal temperature variation with a minimum in February and a maximum in August. Obviously, this coincides with the oscillation of mean temperature in the SSL and the mean of air temperature, which is seen through the strong correlation between the expansion coefficient and air temperature ( $r = 0.94$ ). The extreme low temperature is related to the prolonged period (from 28<sup>th</sup> January to 14<sup>th</sup> February) of Bora wind (ARSO, 2012 a).

EOF analysis reveals that the spatial variation of salinity (Fig. 5c) is explained by the first mode (69%). The highest amplitude signal (1) is seen at the Rižana River mouth. An amplitude signal of 0.8 prevails in the second basin with a value 0.5 at the entrance of the basin ( $13^\circ 44'$ ). In the centre  $\sim 0.2$  and in the shallow part of the BoK, ( $\sim 0.1$ ) lower values can be seen. The expansion coefficient (Fig. 6b) with a minimum on 21<sup>st</sup> March 2013 and a maximum on 13<sup>th</sup> February 2012 has a negative correlation ( $r = -0.79$ ) with the Rižana River daily mean discharge ( $Q$ ), which depicts variability of salinity in relation to variability of the Rižana River discharge.

#### EOF analysis of density and turbidity

The spatial structures of EOF density amplitudes are illustrated in Fig. 7a which shows the high amplitude of density in the second basin. In the first mode of density (Fig. 7a), which explains 73% of all data, the maximal amplitude

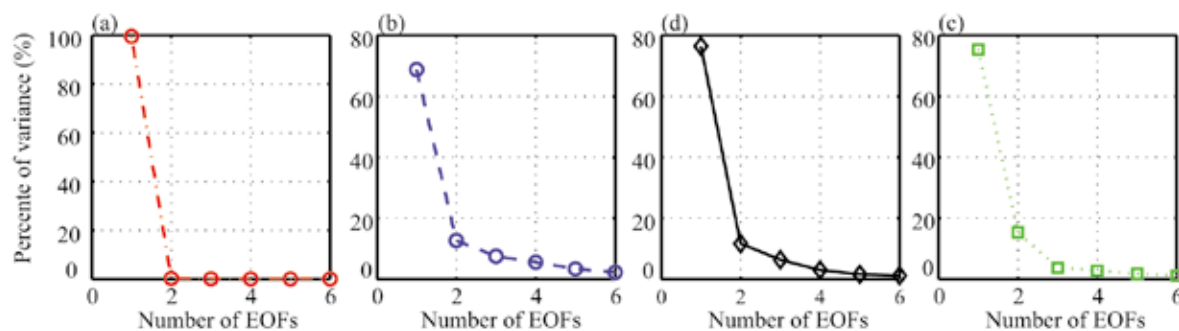


Fig. 4. Percentage of covariance explained by the EOFs of temperature (a), salinity (b), density (c) and turbidity (d)

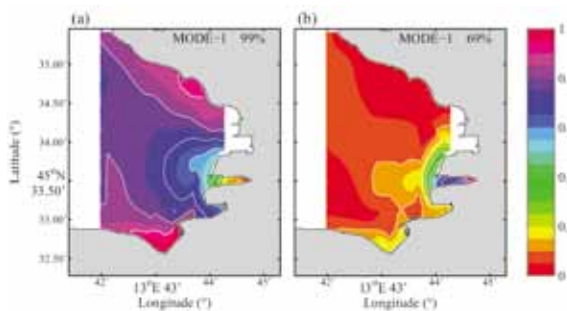


Fig. 5. Normalized maps of the SSL of the first EOF pattern of temperature (a) and salinity (b)

(1) is limited to the Rižana River mouth and to the central part of the second basin, while a signal amplitude of 0.6 is observed at the entrance of the second basin. In the centre of the BoK and adjacent to the coast, the amplitude signal is 0.4. The expansion coefficient (Fig. 8a) is similar to the main expansion coefficient of salinity (Fig. 6b) with a negative correlation coefficient ( $r = -0.79$ ) with the air temperature. The correlation

coefficient with the daily mean discharge of the Rižana River is  $r = 0.25$ . This result suggests that in the studied period the seasonal oscillation of temperature was the primary cause of mean density changes in BoK.

The spatial structure of the first EOF mode (Fig. 7b) of turbidity explains 77% of the data and shows the maximum in the region of the Rižana River mouth. Minima are observed in the western part and in the shallow part of the BoK ( $\sim 0$ ). In the centre of the bay, the value  $\sim 0.5$  was observed. The spatial structure of the signal has minima at the north, west and south sides ( $\sim 0$ ), in the centre of the bay ( $\sim 0.4$ ) and near the Rižana River mouth ( $\sim 1$ ). On 8<sup>th</sup> June 2011, in the proximity of the Rižana River mouth, at sampling site 24 (Fig. 1), the observed turbidity variation value lies between the minimum value of 2 NTU and maximum 120 NTU. The maximum turbidity amplitude was observed in concomitance to the event on 8<sup>th</sup> June 2011 when

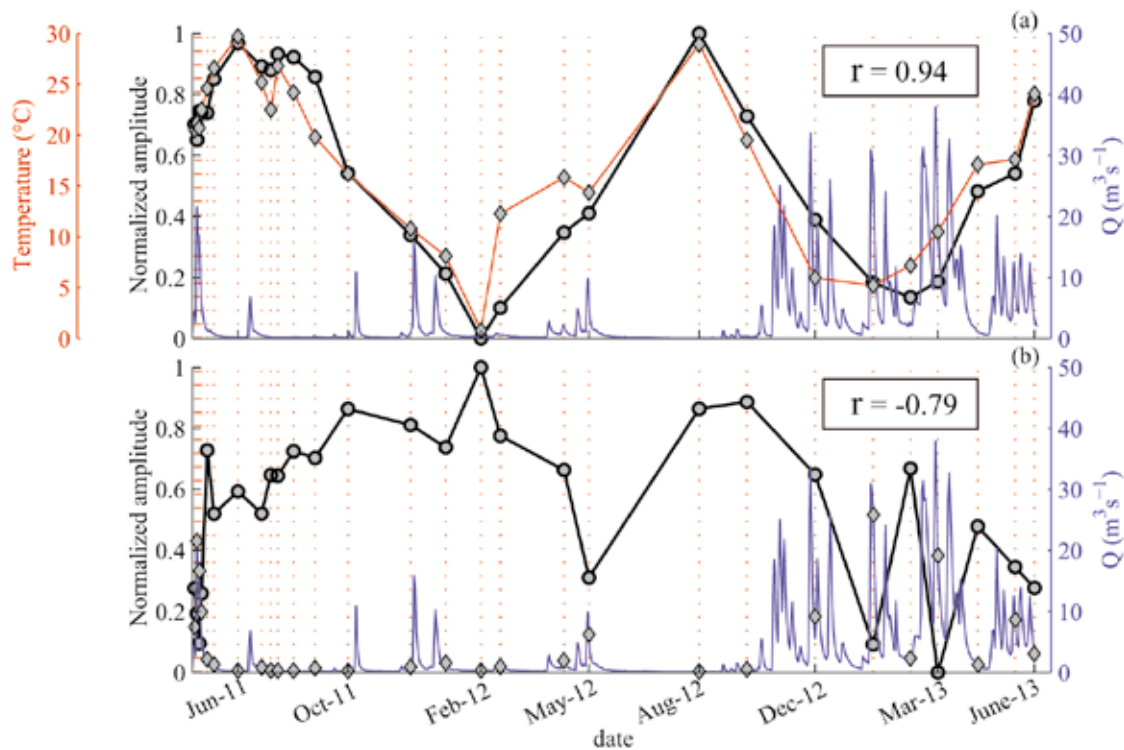


Fig. 6. Normalized expansion coefficients for the SSL of the first EOF mode of temperature (a) and salinity (b). The red line with diamonds represents the air temperature recorded in the port zone. The red dotted stripes denote the survey campaigns and the blue line depicts the Rižana River discharge. The correlation coefficient ( $r$ ) for the mean air temperature and the expansion coefficient of temperature (a) and daily mean river discharge and the expansion coefficient of salinity (b)

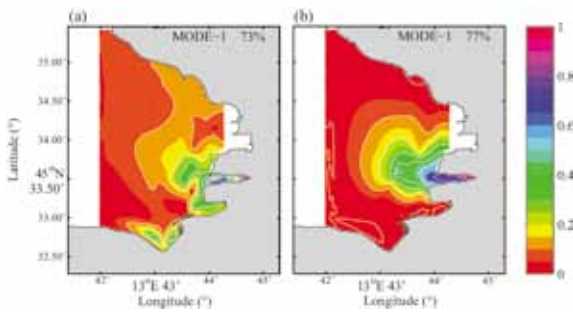


Fig. 7. Normalized maps of the SSL of the first EOF pattern of density (a) and turbidity (b)

2013 ( $50 \text{ m}^3\text{s}^{-1}$ ). The influence of the discharged fluvial water quantity prior to the survey (21<sup>st</sup> March 2013) was accentuated more by the salinity expansion coefficient (Fig. 6b) than by turbidity (Fig. 8b). This difference occurs due to TSS settling and hence lower turbidity while salinity is expected to be more persistent in the SSL. The influence of Rižana River discharge on turbidity is also noticeable in the relatively lower correlation coefficient ( $r = 0.67$ ) in comparison to the salinity.

the highest river outflow of the Rižana River ( $31 \text{ m}^3\text{s}^{-1}$ ) during the entire survey campaign was recorded. Further maximal amplitudes of the expansion coefficient were observed on 23<sup>rd</sup> January 2013 ( $1.8 \text{ m}^3\text{s}^{-1}$ ) and 21<sup>st</sup> March 2013 ( $8.8 \text{ m}^3\text{s}^{-1}$ ). Between 14<sup>th</sup> March 2013 and 20<sup>th</sup> March 2013 the mean flow rate was  $\sim 19.8 \text{ m}^3\text{s}^{-1}$ ; the maximum value was observed on 18<sup>th</sup> March

### Coupled fields analysis

In order to identify the correlations between salinity and turbidity and density and turbidity, the coupled field technique was applied to the first modes. The analysis showed a high square covariance fraction (SCF) that specifies the data explained in the first mode. Turbidity and

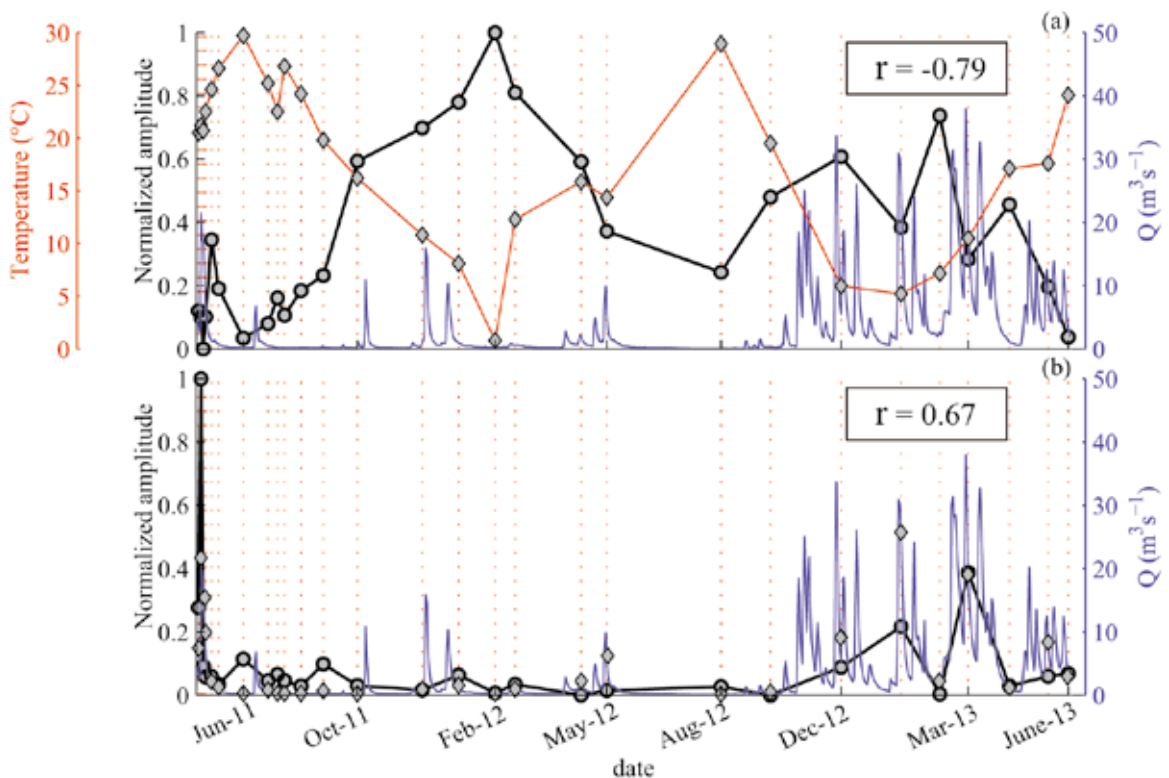


Fig. 8. Normalized expansion coefficients for the SSL of the first EOF mode of density (a) and turbidity (b). The red line with diamonds represents the air temperature recorded in the port zone. The red dotted stripes denote the survey campaigns and the blue line depicts the Rižana River discharge. The correlation coefficient ( $r$ ) for the mean air temperature and the expansion coefficient of density (a) and daily mean river discharge and the expansion coefficient of turbidity (b)

salinity showed  $SCF = 94\%$  and turbidity and density  $SCF = 88\%$ . The strength of coupling (BJÖRNSSON & VENEGAS, 1997) is explained by the correlation coefficient ( $r$ ), which is 0.58 for turbidity and salinity, while for turbidity and density it was somewhat lower (0.42). The maps and expansion coefficients were normalized and plotted as homogenous and heterogeneous, respectively. According to BRETHERTON *et al.* (1992), the left heterogeneous correlation map (turbidity) (Fig. 9c, Fig. 10c) is correlated to the right expansion coefficient (salinity) (Fig. 11a) and thus the turbidity can be estimated from the expansion coefficient obtained from the salinity/density field. The left homogeneous correlation map (Fig. 9a, Fig. 10a) is an indicator of the geographical localization of the covarying part of the analysed field (BRETHERTON *et al.*, 1992).

### Coupled fields analysis of turbidity and salinity

The square covariance in the first mode is evaluated to 94%, while the coupling expansion coefficient is in the correlation value  $r = 0.58$ . The turbidity spatial structure (Fig. 9a) is dominated by the minima signal ( $\sim 0$ ) over the bay. In front of the second basin the signal strength is 0.3 and increases towards the centre (0.6) with maximum amplitude (1) in the Rižana River mouth. A similarly high signal is found in the second basin in the salinity distribution (Fig. 9b). The lower amplitude signal ( $< 0.5$ ) shows a different distribution in comparison to the turbidity indicating poor correlation in this area. The turbidity heterogeneous maps (Fig. 9c) show a range of signal reaching  $\sim 2.5$  km from the Rižana River mouth towards the centre of the BoK. The salinity signal (Fig. 9d) is accentuated relative to that on the homogeneous map (Fig. 9b). However, in the northern part, a minimal signal (0.2) is present in the centre of the bay (0.4). The highest signal is observed at the entrance and within the second basin (0.8 – 1), corresponding to the amplitude (1) of the signal of the turbidity.

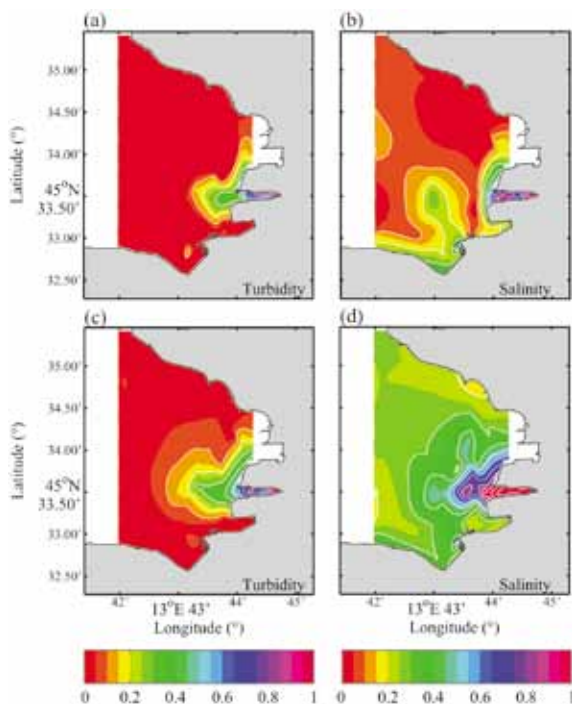


Fig. 9. Normalized SSL homogeneous correlation maps of the first mode of turbidity (a) and salinity (b); and heterogeneous correlation maps of the first mode of turbidity (c) and salinity (d)

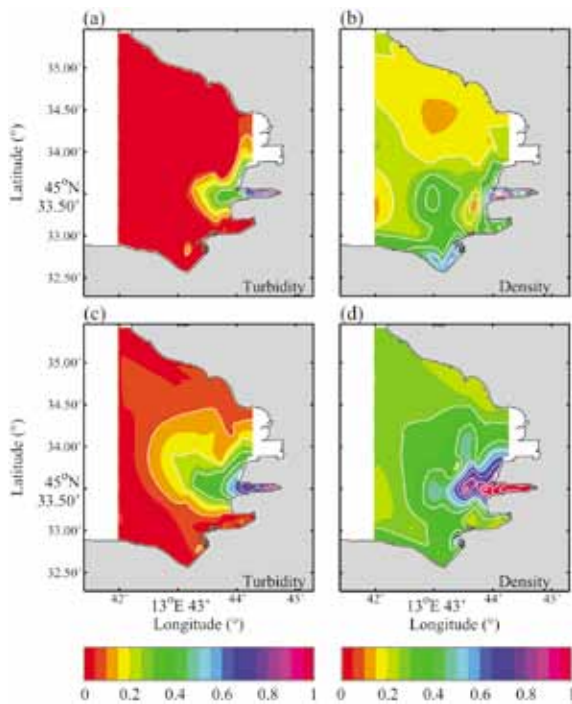


Fig. 10. Normalized homogeneous correlation maps of the first mode SSL turbidity (a) and density (b); heterogeneous correlation maps of the first mode of SSL turbidity (c) and density (d).

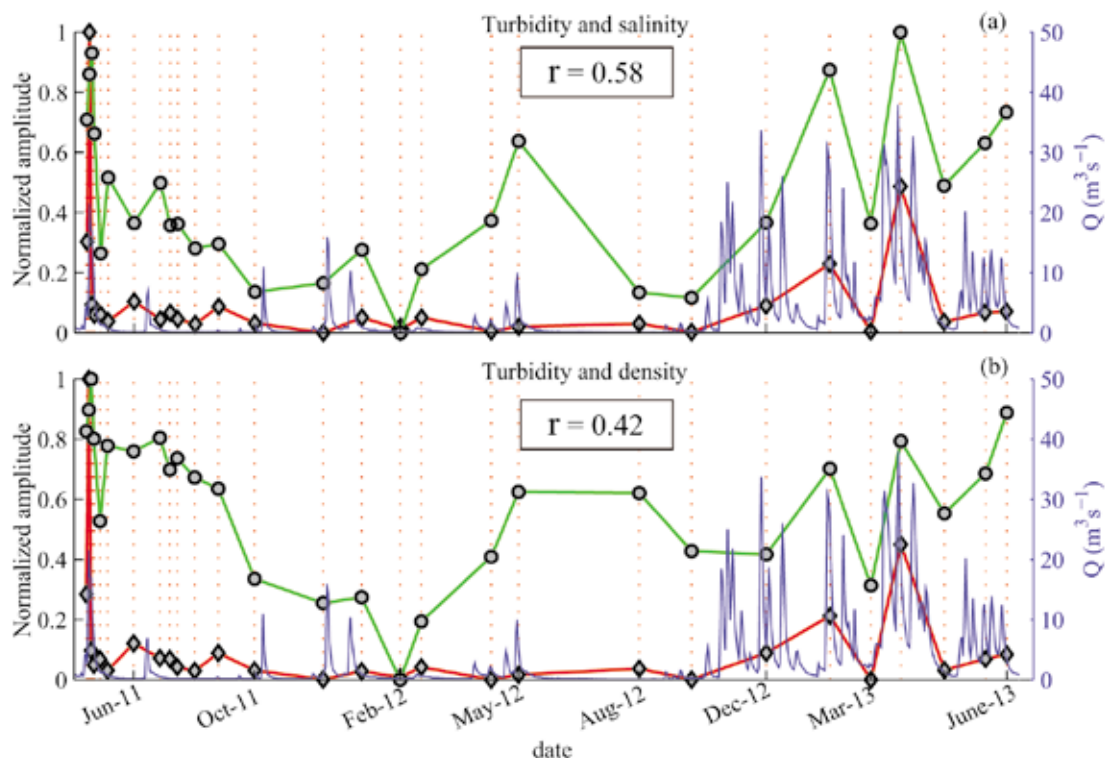


Fig. 11. Normalized expansion coefficient of the first mode of turbidity (circles – green line) and salinity (diamonds – red line) (a) and turbidity (circles – green line) and density (diamonds – red line) (b). The red dotted stripes denote the survey campaigns and the blue line depicts the Rižana River discharge

### Coupled fields analysis of turbidity and density

The square covariance in the first mode is evaluated to 88%, while the coupling expansion coefficient is  $r = 0.42$ . The homogenous map of turbidity (Fig. 10a) shows the same spatial structure of signal as previous analysis (Fig. 9a). The main difference in the correlation maps lies in the maps of density (Fig. 10b, Fig. 10d), which show different spatial structure (Fig. 10b) and higher signal, limited to the entrance and the second basin (Fig. 10d). Higher signal in the turbidity spatial structure is present in the heterogeneous map (Fig. 10c), mainly in the central part of the BoK. The turbidity signal extends from the second basin to the central and northern parts of the bay, where the signal is 0.3, in the centre 0.4 and, in the second basin, 0.6, increasing to its maximum value (1) in the Rižana River mouth.

### Factor analysis

Factor analysis was applied in the three vertical profiles (Fig. 12) recorded at survey sites 5, 19 and 24 (see Fig. 1). The main variations of salinity and turbidity were found in the water column between 0 and 2 m depth in profile 24 (Fig. 12) which is located near the Rižana River mouth. Profile 9 located in the central part of the BoK shows low mean variation in the same layer (0–2 m) while profile 5 located in the open part of BoK showed the lowest mean variation of all variables.

The factor analysis results indicate an opposite correlation of principal components (PC), that together (PC1 and PC2) explain 99% of all the data. The analysis of the selected episodes (Fig. 13) shows the relation between low salinity (due to river discharge) and increased turbidity in the profiles (Fig. 12). The main difference between factor loadings (FL), the salinity and turbidity profiles, was found during high river discharge (8<sup>th</sup> June 2011 and 21<sup>st</sup> March 2013).

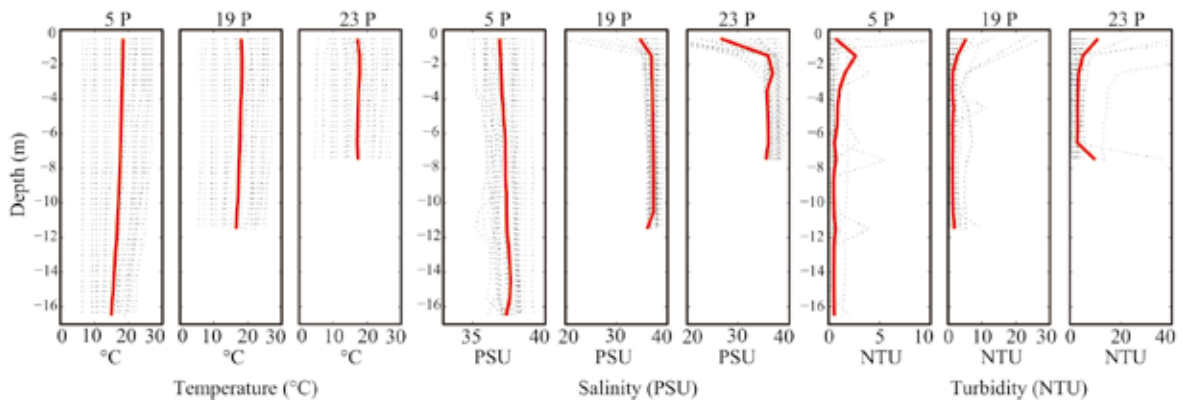


Fig. 12. Temperature, salinity and turbidity profiles at sampling sites 5, 19 and 24. Red (bold) lines show the mean values and black dots the measured profile

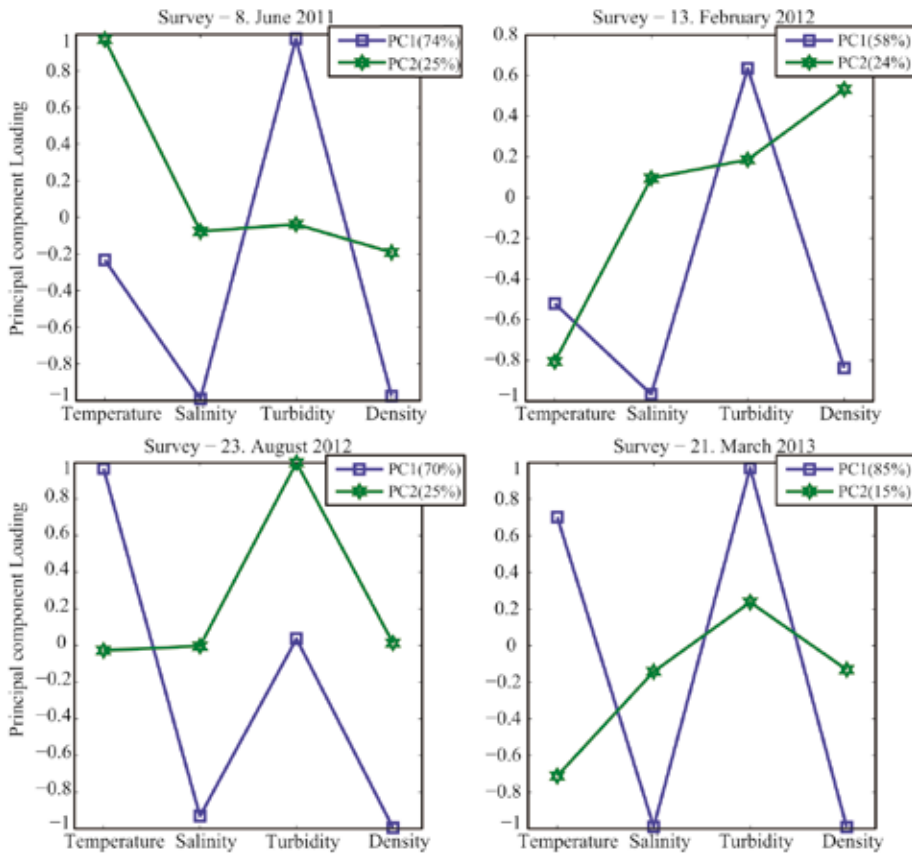


Fig. 13. Factor loadings of temperature, salinity, turbidity and density in the profiles at sampling sites 5, 19 and 24

Minor differences were found on 13<sup>th</sup> February 2012 and 23<sup>rd</sup> August 2012, sharing (74%) and (85%) of all data, respectively. Factor analysis confirms fresh water inputs related to low salinity in connection with density and increased turbidity data. In fact, the results for 8<sup>th</sup> June 2012 and 21<sup>st</sup> March 2013 (Fig. 13) show FL between

salinity (S FL: - 0.95) and turbidity (turbidity FL: 0.97), while density is correlated mainly to salinity ( $\rho$  FL: - 0.91). The minimal difference correlation between salinity and turbidity was observed in the PC1 (70%) on the 23<sup>rd</sup> August 2012 (S FL: - 0.91; turbidity FL: 0), while there was a pronounced difference between tempera-

ture and salinity (FL: 0.96; S FL: - 0.92). The PC2 follows the PC1 with opposite temperature FL (13<sup>th</sup> February 2012, 23<sup>rd</sup> August 2012 and 21<sup>st</sup> March 2013) and less pronounced differences between salinity and turbidity. Salinity and turbidity are regularly counter correlated while density varies in its dependence on temperature (13<sup>th</sup> February 2012 and 8<sup>th</sup> June 2011).

### Turbidity and suspended solids

The correlation between turbidity and TSS concentration data from two environments (river and coastal waters) was analysed through the least squares simple linear regression. The wider range of TSS concentrations were found in both rivers and ranged between 1.04 and 324.61 mg l<sup>-1</sup> and SOM between 0 and 39.22 mg l<sup>-1</sup> representing ~ 35 % of TSS. The high values of TSS concentration were related to high river discharges of the Rižana (33.7 m<sup>3</sup>s<sup>-1</sup>) and Badaševica (3

m<sup>3</sup>s<sup>-1</sup>) (ARSO, 2014 c) during the sampling. Fig. 14a shows all data (n=41) for turbidity and TSS concentration for rivers Rižana and Badaševica with a linear regression model. The model shows a strong linear relationship between turbidity and TSS with a correlation coefficient of R=0.99 and an intercept of - 0.63. The high correlation coefficient is related to the two outliers < 100 NTU and mg l<sup>-1</sup>. The correlation in the river was tested in the lower range of the TSS concentrations (0 – 40 mg l<sup>-1</sup>) and turbidity (0 – 40 NTU) (Fig. 14c). In this range the distribution of the two variables suggests a lower linear relationship in comparison to the larger range (Fig. 14a). However, the correlation coefficient R = 0.92 supports linear dependency with a lower slope (0.77) and higher intercept (1) in the linear model. The turbidity–SOM correlation coefficient for the Rižana and Badaševica Rivers (Fig. 14d) was found to be high (R=0.98) with an intercept of about 0.69 mg l<sup>-1</sup> represent-

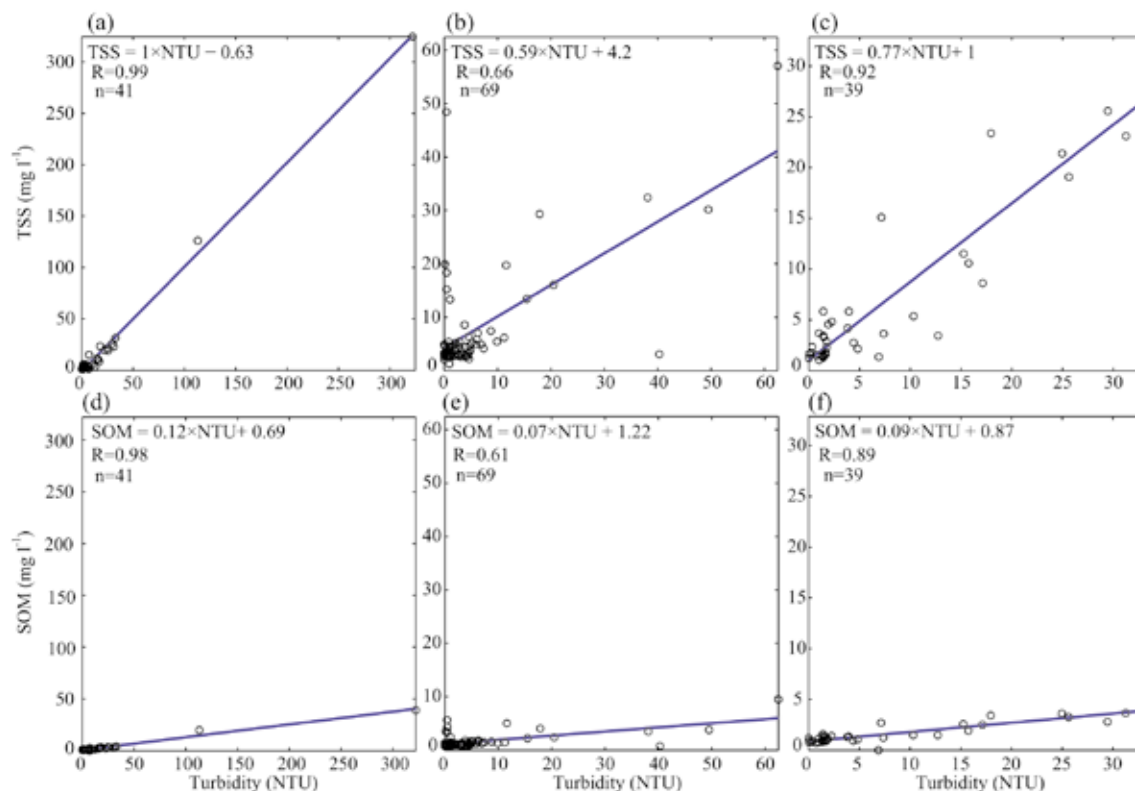


Fig. 14. Regression model for: (a) TSS and turbidity in rivers, (b) TSS and turbidity in coastal waters, (c) TSS and turbidity in rivers in the lower range, (d) SOM and turbidity in rivers, (e) SOM and turbidity in coastal waters, SOM and turbidity in rivers in the lower range

ing SOM which is supposed to be unaffected by light absorbance. This is consistent with a high correlation of TSS with SOM ( $R=0.98$ ) representing on average about 35% of TSS. The turbidity–SOM correlation in the lower range (0 – 40 NTU and  $\text{mg l}^{-1}$ ) in the rivers (Fig. 14f) showed a linear distribution of the two variables with a correlation coefficient (0.89) that is comparable with the model in the large range (Fig. 14d). At the marine sampling sites including the Rižana River mouth, TSS ranged between 1.25 and 57.08  $\text{mg l}^{-1}$  while SOM varied between 0.66 and 9.53  $\text{mg l}^{-1}$  representing about ~ 25% of TSS. All measured values of TSS concentration agreed well to those previously reported in the BoK (OGORELEC *et al.*, 1987). The marine samples showed lower TSS concentration in comparison to the rivers which is probably due to dilution and settling of the sediment in the Rižana River mouth. Fig. 14b plots all sea water data ( $n=69$ ) of turbidity and TSS with a simple linear regression model showing a low correlation ( $R=0.66$ ). This low correlation can be attributed to several factors that include the impact of size, shape and composition of particles and the organic matter that affects turbidity measurements (CLIFFORD *et al.*, 1995; GIPPEL, 1989). The turbidity-SOM correlation for sea water samples (Fig. 14e) was rather low ( $R=0.61$ ) with an intercept of 1.22  $\text{mg l}^{-1}$  representing rather high SOM concentration unaffected by light absorbance. The impact of water colour due to dissolved organic matter (MALCOM, 1985) is evident at low TSS concentrations and higher turbidity which indicates the limitations of the in-situ turbidity measurements.

## CONCLUSIONS

The results demonstrate the application of the spatially extended survey strategy and the statistical data analysis techniques, providing new insights into the spatial and temporal influence of small rivers on the SSL of a shallow bay, the BoK as a study case. The EOF analysis demonstrated single variable spatio-temporal behaviour in the studied period and confirms that the region of fresh water influence is limited to the second port basin and the area ~2.5 km from the Rižana River mouth. The temperature

distribution in the SSL was found to be influenced by the river discharge, while high variability was observed in the shallow part of the bay. Peaks in temporal variations of SSL salinity and turbidity signals coincide temporally with peak discharges of the Rižana River. Correlation between salinity and turbidity variations was found with couple field analysis pointing out the link between the two spatial structures, which determine the region of fresh water influence and the resulting turbidity distribution. The results of factor analysis confirmed the impact of the riverine water on the turbidity variable in the SSL and exclude other factors affecting high turbidity in the studied vertical profiles. High variability of salinity and turbidity was affected by the river discharge in the water column between 0 and 3 m in the port zone at a distance of ~2.5 km from the Rižana River mouth to the open part of BoK.

During the studied period a single episode of river plume was recorded coinciding with the peak of the river discharge. Surveys in such episodes are difficult to perform due to unpredictable weather and conditions at sea. However, the impact of this episode is evident in the spatio-temporal results and deserves particular research that can be performed using numerical modelling of plume distribution. Results of the present study can be used as a valuable calibration and comparison basis for future modelling of TH and TSS distribution.

Turbidity and TSS concentrations were highly correlated in the Rižana and Badaševica Rivers particularly during high river discharges indicating the useful estimation of TSS concentration and transport from the turbidity and river discharge. The present findings were described in the regression models that can be applied mostly in periods of high river discharge for forecasting the spatial and temporal variability of TSS distribution in semi-enclosed shallow bays. Another factor to be taken into account is the lower correlation of turbidity-TSS in the sea water. In order to obtain a reliable regression model and confidence interval on a wide spectrum of turbidity and TSS concentration, numerous water samples and measurements are required.

Since in situ measurement (CDT - turbidity) is a more cost-effective approach compared to laboratory gravimetric analysis, it is necessary to develop a regression model which will bridge the gap of the logistic problems. This was achieved in the presented study with the developed a regression model that will estimate spatial distribution of TSS concentration in the water column and the related deposition rate from turbidity during a high river discharge in a coastal area. In addition to that, the results of this study are of particular interest for the local port authorities in relation to the accumulation of riverine sediments in maritime canals and port basins.

## ACKNOWLEDGEMENTS

This study was partially financed by the European Union, European Social Fund. We thank the Slovenian Environmental Agency and National Institute of Biology–Marine Biology Station Piran for the meteorological, hydrological, temperature and salinity data. The authors would like to express their gratitude to V. MALAČIČ for valuable suggestions and R. PAIN and T. MUTZ for linguistic corrections to improve the paper. This contribution was greatly improved by the comments and suggestions of two anonymous reviewers.

## REFERENCES

- ARSO. 2012 a. Burja in mraz od 28. januarja do 14. februarja 2012 ter visoko valovanje in nizke temperature morja v prvi polovici februarja 2012 = Bora wind and cold from 28 January to 14 February 2012 and the high waves and low sea temperatures in the first half of February 2012. [http://meteo.arso.gov.si/uploads/probase/www/climate/text/sl/weather\\_events/burja-mraz\\_feb12.pdf](http://meteo.arso.gov.si/uploads/probase/www/climate/text/sl/weather_events/burja-mraz_feb12.pdf). 51 p.
- ARSO. 2014 b. Meteorologic data base, ARSO, <http://meteo.arso.gov.si/met/sl/app/webmet/#webmet==8Sdwx2bhR2cv0WZ0V2bvEG-cw9ydlJWblR3LwVnaz9SYtVmYh9icIFGb t9SaulGdugXbsx3cs9mdl5WahxXYyNGap-ZXZ8tHZv1WYp5mOnMHbvZXZu1WYn-wCchJXYtVGdlJnOn0UQQdSf>.
- ARSO. 2014 c. Hydrological data base, ARSO, [http://vode.arso.gov.si/hidarhiv/pov\\_arhiv\\_tab.php](http://vode.arso.gov.si/hidarhiv/pov_arhiv_tab.php).
- BAJT, O. 2000. Hydrocarbons in sea water and coastal sediments of the Slovenian part of the Gulf of Trieste. *Annales. Series historia naturalis*: 61-66.
- BJÖRNSSON, H. & S. A. VENEGAS. 1997. A Manual for EOF and SVD Analyses of Climatic Data. CCGCR Report No. 97-1. 52 p.
- BRETHERTON, C. S., C. SMITH & J. M. WALLACE. 1992. An Intercomparison of Methods for Finding Coupled Patterns in Climate Data. *J Clim*, 5: 541-560.
- BUONGIORNO NARDELLI, B., S. COLELLA, R. SANTOLERI, M. GUARRACINO & A. KHOLOD. 2010. A re-analysis of Black Sea surface temperature. *J Mar Syst*, 79: 50-64.
- CLIFFORD, N. J., K. S. RICHARDS, R. A. BROWN & S. N. LANE. 1995. Laboratory and field assessment of an infrared turbidity probe and its response to particle size and variation in suspended sediment concentration. *Hydrol Sci J*, 40: 771-791.
- COVELLI, S., R. PIANI, A. ACQUAVITA, S. PREDONZANI & J. FAGANELI. 2007. Transport and dispersion of particulate Hg associated with a river plume in coastal Northern Adriatic environments. *Mar Pollut Bull*, 55: 436-450.
- COZZI, S., C. FALCONI, C. COMICI, B. ČERMELJ, N. KOVAČ, V. TURK & M. GIANI. 2012. Recent evolution of river discharges in the Gulf of Trieste and their potential response to climate changes and anthropogenic pressure. *Est Coast Shelf Sci*, 115: 14-24.
- DELCROIX, T. & C. HÉNIN. 1991. Seasonal and interannual variations of sea surface salinity in the tropical Pacific Ocean. *J. Geophys. Res. C*, 96: 22135-22150.
- DROPPO, I. G. 2001. Rethinking what constitutes suspended sediment. *Hydrological Processes*, 15: 1551-1564.
- FAGANELI, J. & V. TURK. 1989. Behaviour of dissolved organic matter in a small, polluted

- estuary. *Sci. Mar.*, 53: 513-521.
- FOFONOFF, N. P., R. C. MILLARD & UNESCO. 1983. Algorithms for computation of fundamental properties of seawater. Unesco. Paris. 53 pp.
- GIPPEL, C. J. 1989. The use of turbidimeters in suspended sediment research. *Hydrobiologia*, 176-177: 465-480.
- GIPPEL, C. J. 1995. Potential of turbidity monitoring for measuring the transport of suspended solids in streams. *Hydrol. Process.*, 9: 83-97.
- GLOVER, M., J. JENKINS & S. C. DONEY. 2011. Modeling methods for marine science. Cambridge University Press. 588 pp.
- HOFMANN, A. & J. DOMINIK. 1995. Turbidity and mass concentration of suspended matter in lake water: a comparison of two calibration methods. *Aquat. Sci.*, 57: 54-69.
- LEDoux, H. & C. GOLD. 2005. An Efficient Natural Neighbour Interpolation Algorithm for Geoscientific Modelling, *Developments in Spatial Data Handling*. Springer Berlin Heidelberg, pp. 97-108.
- LIPEJ, L., R. TURK & T. MAKOVEC. 2006. Endangered species and habitat types in the Slovenian sea. *Zavod RS za varstvo narave*. Ljubljana. 264 pp.
- LUKA KOPER, D.D. 2011. Environmental report 2009. 83 p.
- LUKA KOPER, D.D. 2013. Pridobili smo sodobno opremo za spremljanje okoljskih vplivov = We have acquired a modern equipment to monitor environmental impacts, LUKA KOPER, d.d., <http://www.luka-kp.si/slo/medijski-koticek/arhiv-novic/2997>.
- MALAIČIČ, V., M. CELIO, B. ČERMELJ, A. BUSSANI & C. COMICI. 2006. Interannual evolution of seasonal thermohaline properties in the Gulf of Trieste (northern Adriatic) 1991–2003. *J. Geophys. Res. B*, 111: 1-16.
- MALAIČIČ, V., U. MARTINČIČ, B. MAVRIČ, O. BAJT, N. KOVAČ & V. BERNETIČ. 2014. Vpliv cirkulacije v široko odprtih zalivih in pomorskega prometa na transport sedimenta : poročilo 11 aplikativnega projekta L2-4147 : študija = Influence of circulation in wide open bays and maritime traffic on sediment transport: report 11 applied project L2 -4147 : study. MBP - NIB Piran. 73 p.
- MALCOM, R. L. 1985. Humic Substances in Soil, Sediment, and Water: Geochemistry, Isolation, and Characterization. John Wiley and Sons. 181 pp.
- MOSETTI, F. 1967. Temperatura e salinità nel golfo di Trieste: risultati di un anno di determinazioni. *Pubblicazioni dell'Osservatorio Geofisico sperimentale Trieste*. Nuova serie, Trieste. 1-6 pp.
- OGORELEC, B., M. MIŠIČ, J. FAGANELI, P. STEGNAR, B. VRIŠER & A. VUKOVIČ. 1987. The recent sediment of the Bay of Koper (Northern Adriatic). *Geologija*, 87-121.
- OGORELEC, B., M. MIŠIČ & J. FAGANELI. 1991. Marine geology of the Gulf of Trieste (northern Adriatic) : sedimentological aspects. *Mar. Geol.*, 99: 79-92.
- ORLANDO BONACA, M., L. LIPEJ & S. ORFANIDIS. 2008. Benthic macrophytes as a tool for delineating, monitoring and assessing ecological status: The case of Slovenian coastal waters. *Mar Pollut Bull*, 56: 666-676.
- ORPIN, A. R., P. V. RIDD, S. THOMAS, K. R. N. ANTHONY, P. MARSHALL & J. OLIVER. 2004. Natural turbidity variability and weather forecasts in risk management of anthropogenic sediment discharge near sensitive environments. *Mar. Pollut. Bull.*, 49: 602-612.
- PACKMAN, J., K. COMINGS & D. BOOTH. 1999. Using Turbidity to Determine Total Suspended Solids in Urbanizing Streams in the Puget Lowlands. *Canadian Water Resources Association*, 158-165.
- PLUT, D. 1980. Geografske značilnosti poplavnega sveta ob Rizani in Badasevici = Geographical characteristics of the areas exposed to inundations in the Rizana and Badasevica rivers system (Slovene Istria). *Geografski zbornik*, 101-153.
- PREISENDORFER, R. W. & C. D. MOBLEY. 1988. Principal component analysis in meteorology and oceanography. Elsevier. Amsterdam. 425 pp.
- PRIMORSKE NOVICE. 2014. V Miših avtomatska vodomerna postaja = in the Miših stands a automatic gauging station, Primorske novice.
- REGIONAL OBALA. 2014. Slovensko morje je bogatejše za novi oceanografski boji = Slovenian sea is richer for the new oceanographic

- buoy, [www.regionaobala.si](http://www.regionaobala.si), ed., <http://www.regionaobala.si/novica/slovensko-morje-je-bogatejse-za-novi-oceanografski-boji>.
- STONE, M. & I. G. DROPPA. 1996. Distribution of lead, copper and zinc in size-fractionated river bed sediment in two agricultural catchments of southern Ontario, Canada. *Environ. Pollut.*, 93: 353-362.
- SUK, N. S., Q. GUO & N. P. PSUTY. 1998. Feasibility of Using a Turbidimeter to Quantify Suspended Solids Concentration in a Tidal Saltmarsh Creek. *Est. Coast. Shelf Sci.*, 46: 383-391.
- TURK, V., O. BAJT, P. MOZETIČ, M. POJE, A. RAMŠAK, M. ŠIŠKO, A. MALEJ & T. MAKOVEC. 2013. Monitoring the water quality of the sea and pollution from the inland in accordance with the Barcelona Convention: Annual Report 2012. Piran, Ljubljana. 31 p.
- WOLANSKI, E. 2007. *Estuarine ecohydrology*. Elsevier. Amsterdam. 168 pp.

Received; 28 February 2014  
Accepted: 16 September 2014

## Riječni upliv na termohalina svojstva, zamućenost i suspendirane tvari u plitkom zaljevu (Koparski zaljev, sjeverni Jadran)

Rok SOCZKA MANDAC<sup>1\*</sup>, Branko BOGUNOVIĆ<sup>2</sup>, Dušan ŽAGAR<sup>3</sup> i Jadran FAGANELI<sup>4</sup>

<sup>1\*</sup> *Harpha sea, d.o.o. Kopar, Čevljarska ulica 8, 6000 Kopar, Slovenija*

<sup>2</sup> *Fakultet Prirodoslovno-matematički i informacijskih tehnologija, Sveučilište Primorska, Glagoljaška 8, 6000 Kopar, Slovenija*

<sup>3</sup> *Fakultet građevinarstva i geodetskog inženjerstva, Sveučilite u Ljubljani, Jamova cesta 2, p.p. 3422, 1000 Ljubljana, Slovenija*

<sup>4</sup> *Nacionalni institut za biologiju, Fornače 41, 6330 Piran, Slovenija*

*\*Kontakt adresa, e-mail: rok@harphasea.si*

### SAŽETAK

Utjecaj riječnog upliva na prostorne i vremenske varijabilnosti, termohalina svojstva i mutnoće na morskoj površini (0,5 m) je istraživano u plitkom Koparskom zaljevu (Trščanski zaljev, sjeverni Jadran), koji je pod utjecajem uglavnom zagađene rijeke Rižana.

Vodljivost, temperatura i mutnoća su mjereni mjesečno na 36 postaja između lipnja 2011. i lipnja 2013. Primijenjena je analiza empirijske ortogonalne funkcije (EOF) kako bi se istražili podaci i utvrdio prostorni raspored varijabilnosti, te vremenske promjene temperature, slanosti, gustoće i zamućenosti. Rezultati dobiveni EOF metodom su pokazali visoka odstupanja za sve varijable u području blizu ušća rijeke Rižana.

Visoke varijacije u vremenskoj seriji za sve varijable su pokazala da se uglavnom odnose na visoke varijacije u vremenskom nizu riječnog dotoka. Združena analiza terenskih istraživanja pokazala je da se radi o području niske slanosti i visoke zamućenosti.

Jaka veza je pronađena između zamućenosti i koncentracije suspendiranih krutih tvari (TSS), dok podaci prikupljeni u lokalnim rijekama i u neposrednoj blizini obale upućuju na to da se zamućenost može koristiti kao zadovoljavajući surogat za TSS procjene.

**Ključne riječi:** riječni upliv, termohalina svojstva, zamućenost, suspendirane tvari, sjeverni Jadran